Inorg. Chem. **2005**, *44*, 5212–5221

One-Electron Reduction of Aqueous Nitric Oxide: A Mechanistic Revision

Sergei V. Lymar,*,† Vladimir Shafirovich,‡ and Gregory A. Poskrebyshev†,§

Chemistry Department, Brookhaven National Laboratory, Upton, New York 11973, and Chemistry Department and Radiation and Solid State Laboratory, New York University, New York, New York 10003

Received January 26, 2005

The pulse radiolysis of aqueous NO has been reinvestigated, the variances with the prior studies are discussed, and a mechanistic revision is suggested. Both the hydrated electron and the hydrogen atom reduce NO to yield the ground-state triplet $^3NO^-$ and singlet ^1HNO, respectively, which further react with NO to produce the $N_2O_2^-$ radical, albeit with the very different specific rates, $k(^3NO^- + NO) = (3.0 \pm 0.8) \times 10^9$ and $k(^1HNO + NO) = (5.8 \pm 0.2) \times 10^6$ M^{-1} s^{-1}. These reactions occur much more rapidly than the spin-forbidden acid–base equilibration of $^3NO^-$ and ^1HNO under all experimentally accessible conditions. As a result, $^3NO^-$ and ^1HNO give rise to two reaction pathways that are well separated in time but lead to the same intermediates and products. The $N_2O_2^-$ radical extremely rapidly acquires another NO, $k(N_2O_2^- + NO) = (5.4 \pm 1.4) \times 10^9$ M^{-1} s^{-1}, producing the closed-shell $N_3O_3^-$ anion, which unimolecularly decays to the final $N_2O + NO_2^-$ products with a rate constant of $\sim$300 s^{-1}. Contrary to the previous belief, $N_2O_2^-$ is stable with respect to NO elimination, and so is $N_3O_3^-$. The optical spectra of all intermediates have also been reevaluated. The only intermediate whose spectrum can be cleanly observed in the pulse radiolysis experiments is the $N_3O_3^-$ anion ($\lambda_{max} = 380$ nm, $\epsilon_{max} = 3.76 \times 10^3$ M^{-1} cm^{-1}). The spectra previously assigned to the NO^- anion and to the $N_2O_2^-$ radical are due, in fact, to a mixture of species (mainly $N_2O_2^-$ and $N_3O_3^-$) and to the $N_3O_3^-$ anion, respectively. Spectral and kinetic evidence suggests that the same reactions occur when $^3NO^-$ and ^1HNO are generated by photolysis of the monoprotonated anion of Angeli's salt, $HN_2O_3^-$, in NO-containing solutions.

Introduction

In the early 1970s, two research groups independently investigated the pulse radiolysis of aqueous nitric oxide (NO) and found that, being a free radical, NO rapidly adds to all three primary radicals from water radiolysis (OH radical, hydrated electron, and hydrogen atom).[1,2] Reaction with OH is of little interest, for it directly yields nitrite, which is unreactive toward NO. In contrast, the reactions with hydrogen atom and hydrated electron generate HNO (known as nitroxyl) and NO^- species, respectively, which have been shown to further react with NO to ultimately yield nitrous oxide and nitrite. A complex mechanism for this process has been devised that invokes the intermediacy of the hyponitrite radicals (HN_2O_2 and $N_2O_2^-$) and nitrosohyponitrite molecular species (HN_3O_3 and $N_3O_3^-$), as shown in Figure 1. Both qualitatively and quantitatively, this mechanism is very much dependent on the correct spectral identification of the transients, and Figure 2 shows the assignments that have been made on the basis of the pulse radiolysis data. Barring minor differences, the two groups of researchers have largely agreed on the spectra of intermediates, mechanism, rates of reactions, and equilibrium constants. It is thus not surprising that these conclusions have been widely accepted and have made their way into the spectral[3] and kinetic[4,5] compilations, a number of reviews,[6–9] and the estimates of the redox potentials for the several intermediates in Figure 1.[10,11]

* To whom correspondence should be addressed. Tel.: 631-344-4333. Fax: 631-344-5815. E-mail: lymar@bnl.gov.
† Brookhaven National Laboratory.
‡ New York University.
§ On leave from the Institute of Energy Problems of Chemical Physics, Russian Academy of Sciences, Moscow 117829, Russia.

(1) Grätzel, M.; Taniguchi, S.; Henglein, A. *Ber. Bunsen-Ges. Phys. Chem.* **1970**, *74*, 1003−1010.
(2) Seddon, W. A.; Fletcher, J. W.; Sopchyshyn, F. C. *Can. J. Chem.* **1973**, *51*, 1123−1130.
(3) Hug, G. L. *Optical Spectra of Nonmetallic Inorganic Transients in Aqueous Solution*; National Standard Reference Data Series NSRDS-NBS 69; U.S. Goverment Printing Office: Washington, D.C., 1981.
(4) Neta, P.; Huie, R. E.; Ross, A. B. *J. Phys. Chem. Ref. Data* **1988**, *17*, 1027−1284.

10.1021/ic0501317 CCC: $30.25
Published on Web 05/04/2005

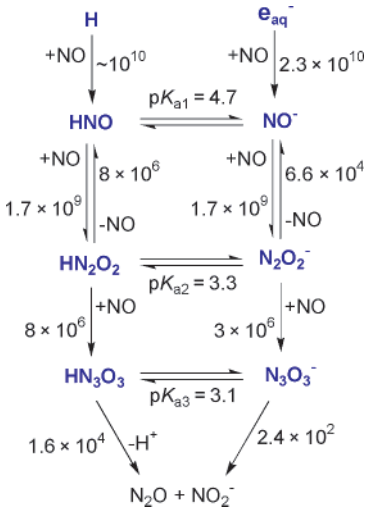

Figure 1. Reactions associated with the capture of hydrogen atom and hydrated electron by NO in solution, as previously proposed by Grätzel and co-workers[1] and by Seddon and co-workers.[2]

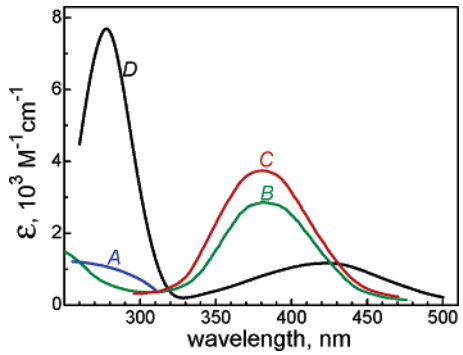

Figure 2. Absorption spectra of transients involved in NO reduction in water. Spectra A−C obtained from pulse radiolysis experiments with NO solutions are adapted from Seddon and co-workers[2] and have been attributed to the NO^- anion (A), $N_2O_2^-$ radical (B), and $N_3O_3^-$ anion (C) by these and the other[1] authors. Spectrum D has been assigned to the $N_2O_2^-$ radical produced by the one-electron oxidation of hyponitrite ($N_2O_2^{2-}$) by OH or N_3 radicals, as described in our recent work.[17] The original papers should be consulted for details.

About two decades later, interest in this chemistry was strongly rekindled by the recognition of NO as a vital biological molecule and by a growing appreciation for the idea that nitroxyl might also play a role in the biochemistry associated with NO. Although there still is no indisputable evidence for the latter, it is difficult to imagine that HNO, which is just one electron away from NO, cannot beget NO and vice versa. Unlike NO, HNO is unstable[12,13] and cannot be prepared and stored for studies. It must be generated in situ, and most investigations dealing with the chemistry and biochemistry of nitroxyl have employed the monoprotonated anion of Angeli's salt ($HN_2O_3^-$) for slow release of HNO into various environments. In a number of cases, it has been found difficult, if not impossible, to quantitatively rationalize the observed reactivity patterns and product distributions on the basis of the mechanism in Figure 1; particularly troublesome has been the low pK_a of 4.7 previously ascribed to HNO from the pulse radiolysis experiments.

Recently, we have began a reevaluation of the thermodynamics and reactivity of nitroxyl and have concluded that: (i) HNO and NO^- have different multiplicities in their ground states, a singlet for HNO and a triplet for NO^-, and (ii) HNO is a very weak acid with pK_a(^{1}HNO = $^3NO^- + H^+$) ≈ 11.4.[13] Essentially the same conclusions have been made independently from ab initio computations by Fukuto, Houk, and co-workers.[14,15] This new pK_a value is 7 units higher than the one derived in the early pulse radiolysis work (Figure 1) that gave no consideration to the degeneracy of the HOMO in NO^-, which leads to a triplet ground state. Further, using flash photolysis of Angeli's salt solutions to produce ^{1}HNO and $^3NO^-$, we have shown that, because of the spin prohibition, the acid−base equilibration of these species occurs so slowly that, unlike in Figure 1, ^{1}HNO and $^3NO^-$ cannot be considered as being in equilibrium during their reactions with NO under any meaningful experimental conditions.[13,16] In that work, we also observed a ca. 300 times lower rate constant for NO addition to HNO and at least 750 times higher rate constant for NO addition to $N_2O_2^-$ than the corresponding values shown in Figure 1. Finally, using pulse radiolysis, we generated the $N_2O_2^-$ radical by the one-electron oxidation of hyponitrite ($N_2O_2^{2-}$) in NO-free solutions[17] and found that the radical absorption spectrum differs dramatically from that attributed to $N_2O_2^-$ by Grätzel and co-workers[1] and by Seddon and co-workers[2] (cf. spectra B and D in Figure 2). Moreover, we have found no evidence for the dissociation of NO from either $N_2O_2^-$ or HN_2O_2 radicals and concluded that these radicals are at least 3 orders of magnitude more stable toward dissociation than the corresponding forward and reverse rate constants in Figure 1 would suggest.

Recognizing that the existence of two mutually exclusive mechanisms and the attendant sets of spectra and rate constants would leave the literature in an untenable state, we have reinvestigated the pulse radiolysis of aqueous NO. Here, we report the results, reconcile all observations, and present a unified mechanism that accounts for the unusual spin states of the NO reduction products. We also present new data on the flash photolysis of Angeli's salt in the presence of NO that strongly corroborate the pulse radiolysis

(5) Ross, A. B.; Mallard, W. G.; Helman, W. P.; Buxton, G. V.; Huie, R. E.; Neta, P. *NDRL/NIST Solution Kinetics Database*, version 2.0; National Institute of Standards and Technology: Gaithersburg, MD, 1994.
(6) Bonner, F. T.; Hughes, M. N. *Comments Inorg. Chem.* **1988**, *7*, 215−234.
(7) Bonner, F. T.; Stedman, G. In *Methods in Nitric Oxide Research*; Feelisch, M., Stamler, J. S., Eds.; Wiley: Chichester, U.K., 1996; pp 3−18.
(8) Hughes, M. N. *Biochim. Biophys. Acta* **1999**, *1411*, 263−272.
(9) Jay-Gerin, J. P.; Ferradini, C. *Biochimie* **2000**, *82*, 161−166.
(10) Stanbury, D. M. *Adv. Inorg. Chem.* **1989**, *33*, 69−138.
(11) Koppenol, W. H. *Methods Enzymol.* **1996**, *268*, 7−12.
(12) Bazylinski, D. A.; Hollocher, T. C. *Inorg. Chem.* **1985**, *24*, 4285−4288.
(13) Shafirovich, V.; Lymar, S. V. *Proc. Natl. Acad. Sci. U.S.A.* **2002**, *99*, 7340−7345.
(14) Bartberger, M. D.; Fukuto, J. M.; Houk, K. N. *Proc. Natl. Acad. Sci. U.S.A.* **2001**, *98*, 2194−2198.
(15) Bartberger, M. D.; Liu, W.; Ford, E.; Miranda, K. M.; Switzer, C.; Fukuto, J. M.; Farmer, P. J.; Wink, D. A.; Houk, K. N. *Proc. Natl. Acad. Sci. U.S.A.* **2002**, *99*, 10958−10963.
(16) Shafirovich, V.; Lymar, S. V. *J. Am. Chem. Soc.* **2003**, *125*, 6547−6552.
(17) Poskrebyshev, G. A.; Shafirovich, V.; Lymar, S. V. *J. Am. Chem. Soc.* **2004**, *126*, 891−899.

results. Where appropriate, we discuss the origin of the mechanistic variances with the previous studies.

Experimental Section

Analytical-grade buffers and Milli-Q purified (ASTM type I) water were used throughout. Angeli's salt (sodium trioxodinitrate, $Na_2N_2O_3$) from Cayman Chemical was used as received. Compressed 100% nitric oxide and its 4.96% and 1.02% analyzed mixtures with nitrogen obtained from Matheson were either used directly or further diluted with argon by filling an evacuated steel cylinder with the individual compressed gases to the desired partial pressure of NO. In all cases, the gas mixtures were purged of N_2O_3 and NO_2 by passing the gas through a glass frit into a scrubbing column of 40% aqueous KOH and then through water in an all-glass-and-metal home-built apparatus. The apparatus was attached to a 70-mL sample reservoir directly connected to a 2-mL pulse radiolysis cell whose outlet valve was remotely controlled. All solutions and headspaces in the cell, reservoir, and purification apparatus were thoroughly purged with helium prior to switching to nitric oxide, and the whole system was kept under a slight positive pressure at all times during the experiment. The solubility of NO in water was taken as 1.9 mM/atm. A solution in the cell was subjected to pulse radiolysis only once and then replaced with a fresh aliquot from the sample reservoir by gating the cell outlet valve.

Pulse radiolysis was carried out with 2 MeV electrons from a van de Graaff accelerator; pulse widths were mainly in the range 0.06−0.3 μs, corresponding to the radiation doses of 100−770 rad and generating radical concentrations of 0.1−0.8 μM per unit G value. Dosimetry was performed with N_2O-saturated 10 mM KSCN solution using $G\epsilon = 4.87 \times 10^4$ ions (100 eV)$^{-1}$ M^{-1} cm^{-1} for the $(SCN)_2^-$ radical at 472 nm. Three passes of analyzing light through a 2-cm cell were used in the detection optical path. All radiolysis experiments were performed with temperature stabilization at 25 ± 0.5 °C.

The laser flash photolysis systems with flow premixing and its application with the NO-containing solutions, as well as the procedures for Angeli's salt sample preparation and handling, have been described in detail elsewhere.[13,16] All flash photolysis experiments were performed at ambient temperature of 22 ± 2 °C.

Results and Discussion

Pulse Radiolysis. The capture of hydrated electrons (e_{aq}^-) by NO constitutes a radical−radical reaction that is not a subject to spin restrictions. It is therefore reasonable to assume that, as with many other electron acceptors, the nascent electron-capture product is generated in its ground state (we will return to this point later) and write

$$e_{aq}^- + NO \rightarrow {}^3NO^- \quad (1)$$

From the dependence on the NO concentration of the e_{aq}^- absorption decay around 700 nm in 10 mM phosphate at pH 7, we have determined $k_1 = (2.1 \pm 0.1) \times 10^{10}$ M^{-1} s^{-1}, very close to the latest reported value shown in Figure 1.[18] As with the electron, the hydrogen-atom capture should also generate the ground-state product

$$H + NO \rightarrow {}^1HNO \quad (2)$$

It has not been possible to directly determine the rate of this reaction because the species involved do not exhibit sufficient characteristic absorption. Undoubtedly, k_2 should be close to the diffusion-controlled limit, and a rough estimate of $k_2 \approx 2.4 \times 10^{10}$ M^{-1} s^{-1} can be obtained from the approximate ratio $k_2/k(H + NO_2^-) \approx 15$ derived from competition product analysis in the steady-state radiolysis[19] and from the recently remeasured $k(H + NO_2^-) = 1.6 \times 10^9$ M^{-1} s^{-1}.[20,21] This k_2 is about twice the tabulated value.[22]

Shown in Figure 3 is the transient absorption kinetics observed at 1.9 mM NO. This is recorded close to the maxima of two completely different spectra in Figure 2 that have been assigned to the $N_2O_2^-$ radical by the previous workers (spectrum B) and by us (spectrum D). This kinetics is similar to those reported by Grätzel and co-workers[1] and by Seddon and co-workers,[2] who attributed the prompt absorption rise at 380 nm to the very rapid, kinetically unresolved formation of $N_2O_2^-$ radical through the concatenation

$$ {}^3NO^- + NO \rightarrow N_2O_2^- \quad (3)$$

(Here, we have reformulated the originally proposed reaction to reflect the triplet spin state for NO^-.) The slow ensuing absorbance growth has been ascribed to the subsequent conversion of this radical into $N_3O_3^-$ via the addition of another NO radical, that is, the reaction

$$N_2O_2^- + NO \rightarrow N_3O_3^- \quad (4)$$

Finally, the exponential decay of the 380 nm absorption on the millisecond time scale has been attributed to unimolecular decomposition of $N_3O_3^-$ to nitrous oxide and nitrite

$$N_3O_3^- \rightarrow N_2O + NO_2^- \quad (5)$$

In accord with this last assignment, we find that the decay of $N_3O_3^-$ is NO-independent. Its rate constant of $k_5 \approx 300$ s^{-1} (Figure 3) is higher than the 87 s^{-1} reported by Grätzel and co-workers,[1] but it agrees well with 240−330 s^{-1} values measured by Seddon and co-workers.[2,23] Because the pK_a of 4.7 was assigned to HNO and the spin prohibition in its acid dissociation reaction was not recognized by the previous studies, HNO produced in reaction 2 has been treated as fully deprotonated, and its reactivity toward NO has not been considered in neutral solutions.

Although we concur with the explanation for the decay, we suggest a different interpretation for most of what happens

(18) The latest report gives (2.3 ± 0.4) × 10^{10} M^{-1} s^{-1} (Seddon, W. A.; Young, M. J. *Can. J. Chem.* **1970**, *48*, 393), whereas the older value is (3.1 ± 0.2) × 10^{10} M^{-1} s^{-1} (Gordon, S.; Hart, E. J.; Matheson, M. S.; Rabani, J.; Thomas, J. K. *Discuss. Faraday Soc.* **1963**, *36*, 193).

(19) Knight, R. J.; Sutton, J. *Trans. Faraday Soc.* **1967**, *63*, 2628−2639.
(20) Mezyk, S. P.; Bartels, D. M. *J. Phys. Chem. A* **1997**, *101*, 6233−6237.
(21) Lymar, S. V.; Schwarz, H. A.; Czapski, G. *J. Phys. Chem. A* **2002**, *106*, 7245−7250.
(22) The previously tabulated value $k(H + NO) = 1.1 \times 10^{10}$ M^{-1} s^{-1} (Buxton, G. V.; Greenstock, C. L.; Helman, W. P.; Ross, A. B. *J. Phys. Chem. Ref. Data* **1988**, *17*, 513) is also based on $k(H + NO)/k(H + NO_2^-) = 15$, but uses the then-available value $k(H + NO_2^-) = 7.1 \times 10^8$ M^{-1} s^{-1}.
(23) Seddon, W. A.; Young, M. J. *Can. J. Chem.* **1970**, *48*, 393−394.

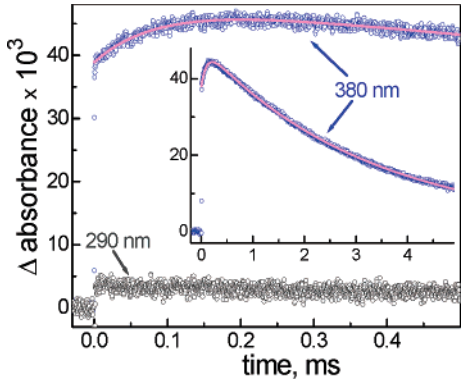

Figure 3. Transient absorption observed at 380 nm (blue) and 290 nm (black) following 0.2-μs radiation pulses (doses 530 ± 10 rad or 0.55 ± 0.01 μM of radicals per unit G value) in 10 mM phosphate at pH 7.0 saturated with 100% NO (1.9 mM). The magenta lines show the two-exponential fits to eq 8 with $k' = 1.1 \times 10^4$ and $k'' = 300$ s^{-1} (main window) and with $k' = 9.5 \times 10^3$ and $k'' = 310$ s^{-1} (inset).

before that. Central to our mechanism is the reevaluation of the highly unusual acid−base equilibrium

$$^1\text{HNO} \rightleftarrows {}^3\text{NO}^- + \text{H}^+ \qquad (6)$$

From our estimate of p$K_a \approx 11.4$ for this reaction,[13] it follows that fully equilibrated nitroxyl should be completely protonated in neutral solutions and, if ^{1}HNO were a normal acid like all other nitrogen acids, the equilibration would be complete in much less than a microsecond. However, we have also shown that, because of the spin prohibition, ^{1}HNO and ^{3}NO$^-$ do not behave as a normal acid−base pair. For instance, the protonation of ^{3}NO$^-$ by water occurs on a millisecond time scale.[13,16] We thus maintain that, even in a fairly concentrated buffer, ^{3}NO$^-$ remains deprotonated during its reaction with NO, a conclusion that we reached earlier on the basis of the behavior of ^{3}NO$^-$ photochemically generated from the Angeli's salt;[13,16] experiments of this kind are discussed in the next section.

Immediately after the pulse in Figure 3, the transient absorbance ratio $\Delta A_{290}/\Delta A_{380}$ is much less than unity, whereas the opposite is expected from the spectrum of authentic $N_2O_2^-$ radical (spectrum D in Figure 2). We therefore suggest that $N_2O_2^-$ radical contributes negligibly to the absorption in Figure 3 and that both 290 and 380 nm signals are due exclusively to the $N_3O_3^-$ anion that has been formed via two independent processes, one occurring within the radiation pulse (prompt rise at $t \approx 0$) and another taking place more slowly after the pulse (ΔA_{380} rise at $0 < t < 0.2$ ms). We also propose that these two steps originate from reactions of ^{3}NO$^-$ and ^{1}HNO, respectively. This interpretation requires that the $N_3O_3^-$ formation through the reaction sequence 3 and 4 occurs about 3 orders of magnitude more rapidly than suggested previously (scheme in Figure 1). Therefore, much better time resolution and/or a much lower concentration of NO than those in Figure 3 are required to actually observe the intermediate $N_2O_2^-$ radical.

Data obtained under such conditions are shown in Figure 4, where the absorbance rise and fall at 290 nm is attributable to the formation and decay of $N_2O_2^-$ during the reaction sequence given by eqs 1, 3, and 4. Before applying a more

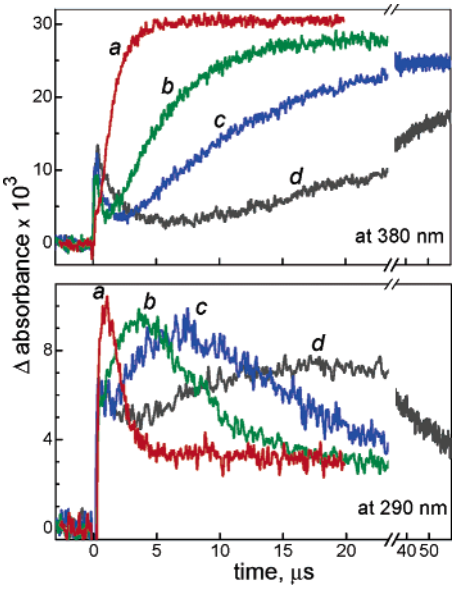

Figure 4. Transient absorption traces recorded at 380 nm (upper panel) and 290 nm (lower panel) upon pulse radiolysis of 10 mM phosphate buffer at pH 7.0 containing 360 μM NO (a, red), 94 μM NO (b, green), 47 μM NO (c, blue), and 19 μM NO (d, black). Radiation doses were 480−750 rad; absorbances are normalized to 500 rad.

rigorous analysis, it is instructive to assume that $k_1 \gg k_3$ and consider only reactions 3 and 4. If the absorptions at 290 and 380 nm were exclusively due to $N_2O_2^-$ and $N_3O_3^-$, respectively, the expected ratio of absorbances $\Delta A_{290}/\Delta A_{380}$ at their maxima is independent of the NO concentration and given by the well-known expression[24]

$$\frac{\Delta A_{290}(t_{max})}{\Delta A_{380}(t_\infty)} = \frac{\epsilon_{290}(N_2O_2^-)}{\epsilon_{380}(N_3O_3^-)}\left(\frac{k_4}{k_3}\right)^{k_4/(k_3-k_4)} \qquad (7)$$

Given that $\epsilon_{290}(N_2O_2^-)/\epsilon_{380}(N_3O_3^-) \approx 1.6$ from spectra C and D in Figure 2 and $\Delta A_{290}(t_{max})/\Delta A_{380}(t_\infty) \approx 0.36$ for all matching pairs of traces in Figure 4, we estimate $k_4 \approx 2k_3$ from eq 7; that is, the addition of the first NO to ^{3}NO$^-$ is significantly slower than the addition of the second NO. A rough estimate of 2.5×10^9 M^{-1} s^{-1} can be made for k_3 from the kinetics at 380 nm in Figure 4; k_4 is then about 5×10^9 M^{-1} s^{-1}.

The kinetic profiles for all species involved in reactions 1, 3, and 4 simulated with these rate constants are shown in Figure 5. Except for expanding or contracting the time scale, the change of NO concentration does not alter these profiles because the rates of all three reactions are first-order in NO. Several observations can be made from a comparison of the calculated and observed kinetics in Figure 5. First, the initial absorbance and its rapid decay are due to e_{aq}^- and reaction 1 at both 290 and 380 nm where the corresponding molar absorptivities of e_{aq}^- are about 800 and 1700 M^{-1} cm^{-1}.[25] Second, the molar absorptivity of ^{3}NO$^-$ is smaller than that of e_{aq}^- at both wavelengths. Third, over 90% of hydrated electrons should have reacted by the time the ^{3}NO$^-$

(24) Espenson, J. H. *Chemical Kinetics and Reaction Mechanisms*; McGraw-Hill: New York, 1981.
(25) Schwarz, H. A. *J. Chem. Educ.* **1981**, *58*, 101−105.

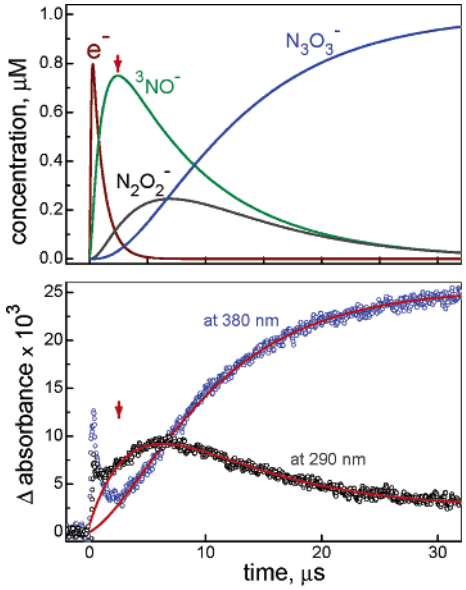

Figure 5. (Upper panel) Simulated kinetics for the transients involved in reaction 1, 3, and 4 with $k_1 = 2.1 \times 10^{10}$, $k_3 = 2.5 \times 10^9$, and $k_4 = 5 \times 10^9$ M^{-1} s^{-1} following a rectangular radiation pulse of 0.2-μs duration that generates 1 μM of e_{aq}^- in solution containing 50 μM of NO. (Lower panel) Transient absorptions observed at 290 nm (near $N_2O_2^-$ maximum, black) and at 380 nm ($N_3O_3^-$ maximum, blue) following a 0.2-μs pulse irradiation (dose 480 rad) of 47 μM NO solution in 10 mM phosphate at pH 7.0. The red lines give fits to eq 8 with $k' = 1.25 \times 10^5$ and $k'' = 2.29 \times 10^5$ s^{-1} for 290 nm and with $k' = 1.32 \times 10^5$ and $k'' = 2.40 \times 10^5$ s^{-1} for 380 nm. Only the portions of traces to the right of the red arrow were used for the fits.

concentration reaches its maximum (indicated by the arrow in Figure 5). From that point on, the absorption change is almost exclusively due to reactions 3 and 4 and can, therefore, be described by the two-exponential function at any wavelength

$$\Delta A(t) = (A_0 - A_2)\exp(-k't) + (A_2 - A_f)\exp(-k''t) + A_f \quad (8)$$

where $k' = k_3[\mathrm{NO}]$; $k'' = k_4[\mathrm{NO}]$; A_0 and A_f are the initial and final absorbances, respectively, at a given wavelength; and A_2 is a parameter whose physical meaning depends on both the observation wavelength and the k'/k'' ratio. As shown in Figure 5, the observed traces can, indeed, be satisfactorily fitted to this equation with essentially the same values for the pair of k' and k'' at both 290 and 380 nm.

We realize that these five-parameter fits, especially applied over a limited range, are not very sensitive and that some statistical analysis with the variation of NO concentration is desirable for obtaining reliable values of k_3 and k_4. Such data are presented in Figure 6, for which multiple transient absorption measurements at the three NO concentrations ranging from 19 to 94 μM have been performed and fitted to eq 8. The statistical analysis shown in Figure 6 yields $k_3 = (3.0 \pm 0.8) \times 10^9$ and $k_4 = (5.4 \pm 1.4) \times 10^9$ M^{-1} s^{-1}; these uncertainties do not include possible systematic error in the NO solubility in the sample solutions. Outside this NO concentration range, the measurements could not be made with our setup: At higher NO concentrations, the reactions are too rapid (e.g., trace at 360 μM in Figure 4); at lower NO concentrations, the pseudo-first-order conditions

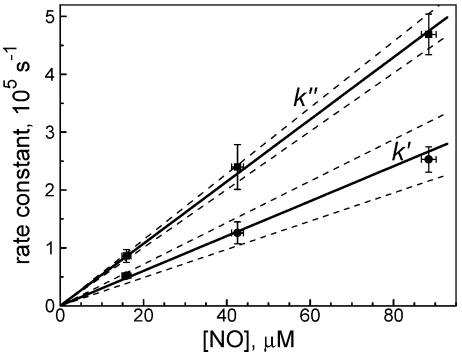

Figure 6. Dependencies on the NO concentration of the apparent rate constants k' and k'' obtained by fitting the transient absorption traces such as those in Figures 4 and 5 to eq 8 as described in the text. Each data point represents the average of 10−20 individual measurements with the error bars displaying the corresponding standard deviations. The NO concentrations calculated from solubility are corrected for NO consumption during the radiation pulse and ensuing reactions; variations around the mean NO concentration values during the time intervals used for fitting to eq 8 are shown as the NO concentration error bars. The solid lines give the linear regressions through the origin using errors as weights, and the dashed lines mark the 95% confidence intervals for the slopes corresponding to $k_3 = (3.0 \pm 0.8) \times 10^9$ and $k_4 = (5.4 \pm 1.4) \times 10^9$ M^{-1} s^{-1}. From lower to higher NO concentration, the average radiation doses are 380, 500, and 640 rad.

could not be maintained because of the large radiation yield of NO consumption that amounts to $G(-\mathrm{NO}) = G(e_{aq}^-) + G(\mathrm{H}) + G(\mathrm{OH}) \approx 6.1$ molecules $(100\ \mathrm{eV})^{-1}$ after the rapid scavenging of all primary radicals and reaches $G(-\mathrm{NO}) = 3G(e_{aq}^-) + G(\mathrm{H}) + G(\mathrm{OH}) \approx 11.5$ molecules $(100\ \mathrm{eV})^{-1}$ by the end of reaction 4. The final NO_2^- and N_2O radiolysis products, appearing both promptly from $\mathrm{OH} + \mathrm{NO} \rightarrow NO_2^- + H^+$ and toward the end from reaction 5, are efficient scavengers of e_{aq}^-, which necessitates the use of fresh sample solution for each kinetic run, a condition that has been thoroughly fulfilled in this study. Even then, dose-dependent corrections of the NO concentrations obtained from solubility are required to account for the NO consumption, both initial by e_{aq}^-, H, and OH and during reactions 3 and 4. In addition, sufficiently small radiation doses have been applied so that promptly appearing nitrite does not significantly interfere. For example, less than 1% of hydrated electrons are expected to react with this nitrite even at the lowest NO concentration in Figure 6.

It is clear from Figure 5 and the above kinetic analysis that the pure spectrum of either $^3NO^-$ or $N_2O_2^-$ cannot be observed at any point in time. What then are spectra A and B in Figure 2 assigned to these species by the previous workers? Shown in Figure 7 are the transient absorption spectra recorded when the 290 nm absorption reaches its maximum (at ~3.5 μs) and well upon completion of reaction 4 (at 50 μs) under reaction conditions that are nearly identical to those used previously for measuring the "NO^- spectrum" in Figure 2 (spectrum A).

First, we note that, in the 250−310 nm region, the NO^- spectrum in Figure 2 resembles our spectrum at 3.5 μs in Figure 7. Second, it is clear from the primary kinetic data presented in the original papers that the time resolution employed was not sufficient to follow the rising portion of absorption around 300 nm;[1,2] only the falling portion of the

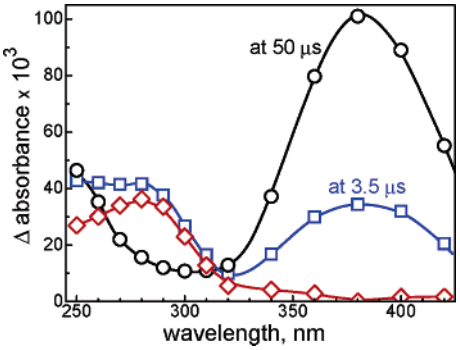

Figure 7. Transient absorption spectra recorded at 3.5 μs (blue squares) and at 50 μs (black circles) following pulse radiolysis (dose 1.7 krad) of 10 mM phosphate buffer at pH 7 containing 94 μM NO. The red diamonds show the difference spectrum obtained by subtracting the 50-μs spectrum from the 3.5-μs spectrum after normalizing the two at 380 nm.

kinetic curve was seen, and the earliest transient spectrum was taken at or slightly past the time when the transient absorption reached its maximum. From that time on, the transient kinetics looks fairly close to single-exponential at all wavelengths, as it should when one of the exponentials in eq 8 becomes small. This deceivingly simple appearance arising from insufficient time resolution is, we believe, the main reason that the reaction sequence 3 and 4 was interpreted as the single reaction 3. Accordingly, the initial and final spectra were assigned to NO^- and $N_2O_2^-$, respectively (Figure 2, spectra A and B). In reality, the spectra of NO^- and $N_2O_2^-$ cannot be cleanly determined from the pulse radiolysis of NO because these species always coexist in solution; most of the time, they also coexist with either $N_3O_3^-$ or e_{aq}^- (see Figure 5), which both absorb. At 50 μs, the reaction sequence 1, 3, and 4 is complete, and the corresponding spectrum in Figure 7 is that of $N_3O_3^-$ ion with possible contribution from ^{1}HNO (produced in reaction 2) that, as described below, has not even begun reacting with NO at that time. This spectrum is practically identical in shape to spectrum B in Figure 2, previously assigned to the $N_2O_2^-$ radical; that is, the data converge, but not the mechanisms. Clearly, the 380 nm band in the 3.5-μs spectrum in Figure 7 is also due mainly to $N_3O_3^-$ that has accumulated by that time. Unfortunately, neither previous research group reported the visible portion of their "NO^- spectrum", so it remains unknown whether they also observed the 380 nm band at their shortest times.

A rough idea about the spectrum of mixed $^3NO^-$ and $N_2O_2^-$ is given by the difference spectrum in Figure 7, which is obtained by subtracting the 50-μs spectrum from the 3.5-μs spectrum after normalizing the two at 380 nm. This procedure somewhat overcorrects for the $N_3O_3^-$ absorption, as it assumes that nothing else absorbs at this wavelength. Nevertheless, the difference spectrum clearly resembles that of authentic $N_2O_2^-$ radical shown by line D in Figure 2; both spectra peak at 280 nm. Clearly, the contribution from $^3NO^-$ to the difference spectrum is not large, even though its concentration is about two times the concentration of $N_2O_2^-$ at 3.5 μs.

Evident in Figure 4 is the increase in signal amplitude with increasing NO concentration, which is attributable to

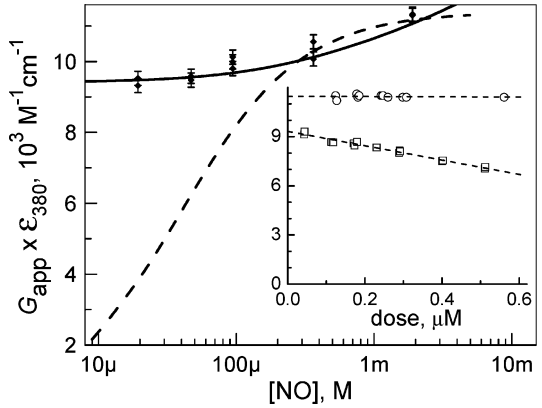

Figure 8. Dependence on the NO concentration of $G_{app}\epsilon_{380}$ measured after the completion of reactions 3 and 4 in neutral phosphate buffered solutions. The solid curve corresponds to eq 9 with $G_0\epsilon_{380} = 9.4 \times 10^3$ M^{-1} cm^{-1} and all the other parameters taken from the work of Bartels and co-workers.[27] The dashed line shows the function $[NO]/(K_{-4} + [NO])$ multiplied by 11.4×10^3 M^{-1} cm^{-1} and represents the expected dependence for $N_3O_3^-$ dissociation with $K_{-4} = 3.9 \times 10^{-5}$ M (see text). The inset gives dependencies of $G_{app}\epsilon_{380}$ on the radiation dose expressed in micromolar units of the radicals generated per radiation pulse per unit G value. Circles, in 1.9 mM NO; squares, in 19 μM NO. The true $G_{app}\epsilon_{380}$ values at various NO concentrations have been obtained by extrapolating the corresponding dose dependencies to zero dose as shown by the dashed straight lines.

the greater radiation yield of transients at large NO concentration. The NO concentration dependence of the apparent values for $G_{app}\epsilon_{380}$ measured when the $N_3O_3^-$ accumulation through reactions 3 and 4 is complete is shown in Figure 8, and its shape is characteristic of radiation spur effects on G_{app}.[26] The increase in yields of electron scavenging (here, reaction 1) commonly becomes significant when the scavenging power, S, exceeds $\sim 10^6$ s^{-1}; in our case, $S = k_1[NO]$, and this occurs at $[NO] > 50$ μM.

To evaluate the spur effects on the electron scavenging yield, it is sufficient to know the time-dependent survival probability, $G_e(t)$, of the radiolytically generated hydrated electrons in pure water; an empirical multiexponential function accurately describing $G_e(t)$ has recently been obtained by Bartels and co-workers.[27] The dependence of G_{app} on the NO concentration can be derived with the help of a Laplace transform of $G_e(t)$, which yields

$$G_{app} = S\int_0^\infty G_e(t)\exp(-St)\,dt = G_0\left(1 + \sum_1^4 C_i\frac{S}{S+\kappa_i}\right) \quad (9)$$

where $S = k_1[NO]$, G_0 is the radiation yield of hydrated electrons that escape the spurs in the absence of NO, and C_i and κ_i are scavenger-independent empirical parameters whose numerical values have been reported.[27] Using these values and $G_0\epsilon_{380}$ as the only adjustable parameter, the experimental NO concentration dependence can be satisfactorily reproduced (solid curve in Figure 8) with $G_0\epsilon_{380} = 9.4 \times 10^3$ M^{-1} cm^{-1}. Accepting the recommended value of $G_0 = 2.5$,[27] we obtain $\epsilon_{380}(N_3O_3^-) = 3.76 \times 10^3$ M^{-1} cm^{-1} for the molar

(26) Buxton, G. V. In *Radiation Chemistry. Principles and Applications*; Farhataziz, R. M. A., Rodgers, M. A. J., Eds.; VCH Publishers: New York, 1987; pp 321−349.
(27) Bartels, D. M.; Cook, A. R.; Mudaliar, M.; Jonah, C. D. *J. Phys. Chem. A* **2000**, *104*, 1686−1691.

absorptivity of the $N_3O_3^-$ ion with less than 5% uncertainty. As shown in the inset to Figure 8, the measured value of $G_{app}\epsilon_{380}$ steeply decrease with radiation dose, but only at low NO concentration. This effect is attributable to the partial loss of e_{aq}^- through homogeneous diffusion-controlled recombination with H and OH, which occurs in competition with the useful reaction 1. The usual procedure of extrapolating to zero dose has been employed to correct for this effect and obtain the true NO concentration dependence of $G_{app}\epsilon_{380}$.

It is important to recognize the origin of the small NO concentration dependence in Figure 8 because a similar dependence was observed by the previous workers,[1,2] albeit for a NO concentration range about 10 times smaller than that used in this work, and was interpreted as evidence for a significant and rapid reversibility of reaction 3. The equilibrium constant $K_{-3} = 3.9 \times 10^{-5}$ M shown in Figure 1 was derived solely from this dependence, and no other evidence for instability of the $N_2O_2^-$ radical with respect to its dissociation back to NO^- and NO has ever been presented. In variance with this view, we have recently demonstrated that K_{-3} does not exceed 10^{-8} M, that is, the $N_2O_2^-$ radical is stable for all practical purposes.[17] Considering the spectral identification of transients described above, we do not have to carry our arguments further than to note that the 380 nm absorption does not belong to $N_2O_2^-$ and thus its NO concentration dependence tells nothing about the properties of $N_2O_2^-$. This absorption actually belongs to $N_3O_3^-$, so the question can only be whether the NO concentration dependence in Figure 8 has to do with the instability of $N_3O_3^-$ with respect to elimination of NO, that is, a rapid equilibration in reaction 4. If this were the case, the functional form of the NO concentration dependence would be [NO]/(K_{-4} + [NO]), and this is plotted as the dashed curve in Figure 8 with the previously suggested value of 3.9×10^{-5} M for the equilibrium constant. Quite obviously, the curve does not fit, and there is no K_{-4} value that would fit, because of the curve shape. We thus conclude that the NO concentration dependence in Figure 8 has nothing to do with the reversibility of either reactions 3 or 4 and that both corresponding dissociation constants are immeasurably low. An upper limit of 10^{-8} M for K_{-3} has been estimated previously,[17] and K_{-4} does not exceed 10^{-6} M based on the fact that the concentration dependence down to ~10 μM in Figure 8 is adequately described in terms of the spur scavenging model alone. (In a forthcoming paper, we will decrease the upper limit for K_{-4} by more than 1 order of magnitude based on a different type of data.)

In discussing Figure 3, we have suggested that the slow absorption rise at 380 nm is also due to $N_3O_3^-$ anion formation that, unlike the prompt rise initiated by $^3NO^-$, originates from ^1HNO produced by the H-atom addition to NO in reaction 2. That is, this $N_3O_3^-$ is made through the rate-determining reaction

$$^1HNO + NO \rightarrow N_2O_2^- + H^+ \qquad (10)$$

followed by the much more rapid reaction 4. Indeed, the amplitude of the slow growth in Figure 3 is about 20% of the prompt amplitude rise, which corresponds to the ratio of radiation yields for e_{aq}^- and H and is consistent with the parallel occurrence of the two independent $N_3O_3^-$ formation processes arising from these two species. The rates for both processes, one due to sequential reaction 1, 3, and 4 and the other due to reactions 2, 10, and 4, depend linearly on the NO concentration and are well separated in time because of the sluggishness of reaction 10. Direct evidence supporting this conclusion can be obtained by using a concentrated acetate buffer near its pK_a, where most of hydrated electrons are converted into H[28]

$$e_{aq}^- + CH_3CO_2H \rightarrow CH_3CO_2^- + H \qquad k_{11} \approx 2 \times 10^8\ M^{-1}\ s^{-1} \qquad (11)$$

before reducing NO. Figure 9 compares the transient kinetics obtained in acetate (0.13 M acetic acid content; about 75% of the hydrated electrons produce H via reaction 11) with the kinetics at the same NO concentration measured in dilute phosphate (all hydrated electrons yield $^3NO^-$). The large increase in amplitude of the H-initiated process at the expense of the e_{aq}^--initiated process is apparent in acetate.

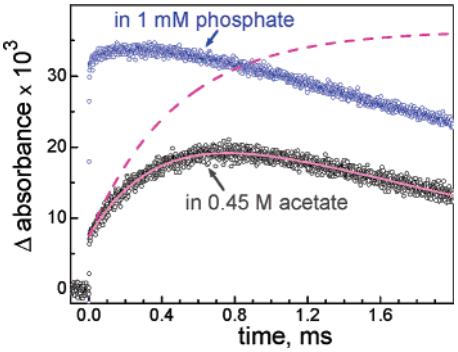

Figure 9. Transient absorption kinetics recorded at 380 nm following pulse radiolysis (dose 500 rad) of 1 mM phosphate at pH 7 (upper blue trace) and 0.45 M acetate at pH 5 (lower black trace; acetic acid content 0.13 M); both contain 0.36 mM NO. The solid magenta line shows a two-exponential fit to eq 8 with $k' = 2.09 \times 10^3\ s^{-1}$, $k'' = 490\ s^{-1}$, $A_0 = 0.0075$, $A_2 = 0.0364$, and $A_f = 0$. The dashed line corresponds to the same equation and parameters, except that $k'' = 0$.

Using the mechanism for $N_3O_3^-$ formation and decay given by the reaction sequence 10, 4, and 5 and considering that $k_4 \gg k_{10}$, eq 8 for the transient absorption applies, with $k' = k_{10}$[NO] and $k'' = k_5$. As seen in Figures 3 and 9, the 380-nm kinetic traces conform well to the predicted two-exponential behavior. By averaging the fitted k' values for 20 traces similar to those in Figure 3 (1.9 mM NO in 10 mM phosphate), we have obtained $k_{10} = (5.77 \pm 0.16) \times 10^6\ M^{-1}\ s^{-1}$, which is in excellent agreement with $k_{10} = (5.81 \pm 0.14) \times 10^6\ M^{-1}\ s^{-1}$ calculated from fitting 12 runs similar to the lower trace in Figure 9 (0.36 mM NO in 0.45 M acetate).

Although nearly the same amounts of electrons plus H atoms have been produced in the two experiments shown in Figure 9, the maximum concentration of $N_3O_3^-$ attained in acetate is some 40% lower than that in phosphate. However, this decrease in yield is only apparent and is due to the decay of $N_3O_3^-$ in parallel with its formation. If the decay were inconsequential, the $N_3O_3^-$ accumulation would follow the

dashed line in Figure 9, which was reconstructed from the fitting parameters for the actual kinetics. In terms of eq 8, the ratio of the slow and prompt amplitudes for this line is $(A_2 - A_0)/A_0 = 3.9$, which closely matches the expected ratio of radiation yields $G(^1HNO)/G(^3NO^-) = [0.75G(e_{aq}^-) + G(H)]/0.25G(e_{aq}^-) = 3.8$ with 1:3 partitioning of hydrated electrons between reactions 1 and 11. This match leaves no doubt that the prompt and slow $N_3O_3^-$ formation processes originate with $^3NO^-$ and ^1HNO, respectively.

Under conditions of Figure 9, about 90% of OH ions react with acetate, producing ~1 μM of the carbon-centered $CH_2CO_2^-$ radical,[28,29] which is expected to form a long-lived C-nitroso closed-shell adduct with NO at a nearly diffusion-controlled rate, as has been observed, for example, for the ethanol radicals.[30] Only if this $ONCH_2CO_2^-$ nitroso species were strongly absorbing at 380 nm could it interfere with the observation of the nitroxyl reactions. However, aliphatic nitroso compounds do not appreciably absorb at wavelengths longer than 300 nm.[30,31] Accordingly, we have found that the transient absorption in Figure 9 decays completely after a few milliseconds, indicating that there is no interference from the radiolytically generated nitrosoacetate.

Laser Flash Photolysis. Recently,[13,16] we suggested that the photochemical N−N bond heterolytic cleavage in the monoprotanated anion of Angeli's salt (hydrogen trioxodinitrate, $HN_2O_3^-$, $pK_a = 9.7$)[32] simultaneously generates both $^3NO^-$ and ^1HNO in an approximately 1:3 proportion

$$HN_2O_3^- (+ h\upsilon) \rightarrow \sim 0.25(^3NO^- + H^+ + NO_2^-) + \sim 0.75(^1HNO + NO_2^-) \quad (12)$$

The mechanism of this photochemical process remains speculative, but the products appear in solution promptly, i.e., they are formed within the UV laser pulse, which gives a convenient, NO-independent method for generating $^3NO^-$ and ^1HNO. We now compare the data obtained using this method with the pulse radiolysis results discussed in the preceding section and show that, indeed, the peculiar stoichiometry of reaction 12 correctly describes the products and their yields.

The transient absorption changes on a short time scale upon flash photolysis of $HN_2O_3^-$ in the presence of NO are shown in Figure 10. They are remarkably similar to the changes induced by the radiolytically generated hydrated electrons in the NO-containing solutions (Figures 4, 5, and 7). The only significant difference is the bleaching observed at $\lambda < 280$ nm caused by consumption of the $HN_2O_3^-$ starting material, which strongly absorbs in this spectral region. The band centered at 380 nm in Figure 10 is similar to that in Figure 7, suggesting the $N_3O_3^-$ anion as the reaction product.

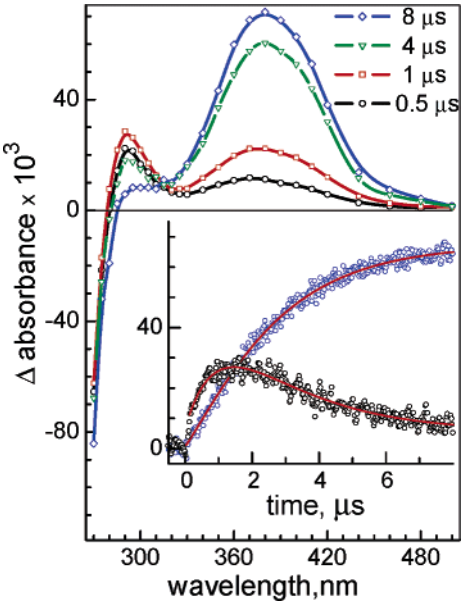

Figure 10. Transient absorption spectra recorded at the indicated delay times after flash photolysis of 0.6 mM $HN_2O_3^-$ in a solution containing 0.18 mM NO at pH 7 (0.1 M phosphate). Inset shows kinetic traces at 290 nm (black) and 380 nm (blue). The red lines give fits to eq 8 with $k' = 4.4 \times 10^5$ and $k'' = 1.0 \times 10^6$ s^{-1}.

As with the pulse radiolysis of NO in Figure 5, the 380 nm absorption increases monotonically, whereas the 290 nm absorption goes through a low maximum (Figure 10, inset). Moreover, the kinetics is well described by eq 8 (which applies for any pair of sequential first-order reactions) with the same $k' = 4.4 \times 10^5$ and $k'' = 1.0 \times 10^6$ s^{-1} at both wavelengths. Dividing this values by [NO] = 0.18 mM in Figure 10, we calculate 2.4×10^9 and 5.6×10^9 M^{-1} s^{-1}, respectively, for the corresponding pair of bimolecular rate constants. These values are virtually identical to the rate constants for the sequential addition of NO to $^3NO^-$ in reactions 3 and 4 obtained in pulse radiolysis experiments (see Figure 6). Thus, at the short time scale following flash photolysis of $HN_2O_3^-$, we observe the same reactions as those initiated by e_{aq}^- in pulse radiolysis of NO solutions and conclude that the $^3NO^-$ anion is indeed among the nascent photolysis reaction products as shown in reaction 12.

On a much longer time scale and at higher NO concentrations than in Figure 10, $N_3O_3^-$ formation by reactions 3 and 4 becomes kinetically unresolved and degenerates into a prompt absorption rise simultaneous with the laser pulse (Figure 11). This rise is followed by a much larger and slower accumulation of $N_3O_3^-$, which eventually decays with a 2.4-ms half-life. This pattern is again similar to our pulse radiolysis observations in Figures 3 and 9; the only difference is in the relative amplitudes for the prompt and slow rises. As with the pulse radiolysis data, the kinetics in Figure 11 is consistent with two sequential reactions and fits well to eq 8. Rate constants for the slow growths (k') and for the final decays (k'') at the same pH and NO concentration in Figures 3 and 11 are virtually identical. In both cases, k'' is independent of the NO concentration, as it should be if it corresponds to reaction 5. The rate constant k' for the rise

(28) Buxton, G. V.; Greenstock, C. L.; Helman, W. P.; Ross, A. B. *J. Phys. Chem. Ref. Data* **1988**, *17*, 513−886.
(29) Fessenden, R. W. *J. Chem. Phys.* **1973**, *58*, 2489−2500.
(30) Czapski, G.; Holcman, J.; Bielski, B. H. J. *J. Am. Chem. Soc.* **1994**, *116*, 11465−11469.
(31) Rao, C. N. R.; Bhaskar, K. R. In *The Chemistry of the Nitro and Nitroso Groups*; Feuer, H., Ed.; Interscience: New York, 1969; Vol. 1, pp 137−163.
(32) Sturrock, P. E.; Ray, J. D.; McDowell, J.; Hunt, H. R. *Inorg. Chem.* **1963**, *2*, 649−650.

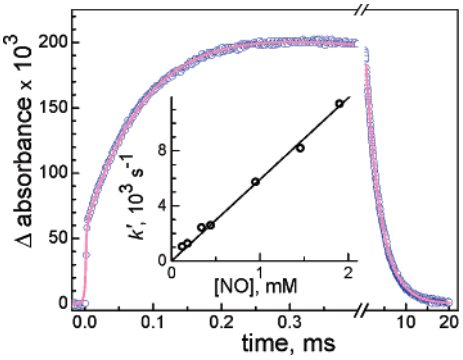

Figure 11. Kinetics recorded at 380 nm after flash photolysis of 0.3 mM $HN_2O_3^-$ in a solution containing 1.9 mM NO at pH 7 (0.1 M phosphate). The time scales are selected to show the slow portion of $N_3O_3^-$ formation and subsequent decay; note the break in the time axis. The solid magenta line is a two-exponential fit to eq 8 with $k' = 1.1 \times 10^4$ s^{-1} and $k'' = 290$ s^{-1}. The inset gives the dependence of k' on the NO concentration and its linear fit through the origin with the slope corresponding to $k_{10} = (5.9 \pm 0.1) \times 10^6$ M^{-1} s^{-1}.

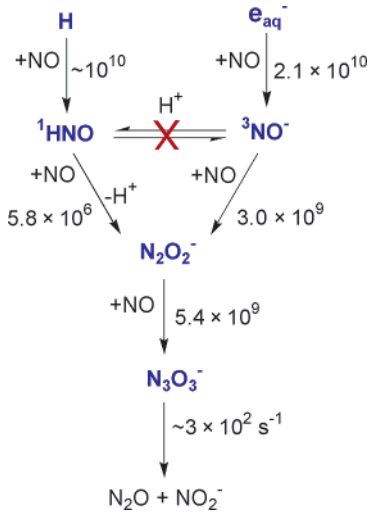

Figure 12. The mechanism for one-electron NO reduction in neutral aqueous solution derived in this work. Except for the one indicated, all rate constants are in M^{-1} s^{-1}.

linearly increases with NO concentration, as seen in Figure 11(inset), from which a bimolecular rate constant of $(5.9 \pm 0.1) \times 10^6$ M^{-1} s^{-1} is obtained, in excellent agreement with $k_{10} = 5.8 \times 10^6$ M^{-1} s^{-1} calculated from Figures 3 and 9. Thus, the slow $N_3O_3^-$ formation in the flash photolysis experiments is initiated by ^{1}HNO photochemically generated in reaction 12. The relative amplitudes of the prompt and slow $N_3O_3^-$ growth processes in Figure 11 are approximately 1:3, which corresponds to the relative amounts of $^3NO^-$ and ^{1}HNO produced in the photochemical step, thus validating the stoichiometry of reaction 12.

Mechanistic Summary. There is sufficient energy to generate both the ground triplet state of NO^- and its excited singlet state as the nascent product of the hydrated-electron capture by NO. However, we have recently presented evidence that, being an extremely strong base with pK_a(^{1}HNO = $^1NO^- + H^+$) $\approx$ 23,[13] the $^1NO^-$ anion is protonated by water within some 0.1 ns producing ^{1}HNO with 96% yield; the remaining 4% of $^1NO^-$ relaxes to $^3NO^-$.[16] Thus, the assumption that the electron capture by NO mainly generates $^1NO^-$ would make ^{1}HNO the major electron-capture product available for further reactions with NO, which is in clear disagreement with the reactivity pattern observed in this work, and we conclude that reaction 1 leading to the ground-state $^3NO^-$ is indeed the major hydrated-electron-capture pathway.

A minimal reaction scheme quantitatively accounting for all observations made with pulse radiolysis of neutral NO solutions is shown in Figure 12. Spectral and kinetic evidence suggests that the same reactions occur when $^3NO^-$ and ^{1}HNO are generated directly by photolysis of the $HN_2O_3^-$ anion in a NO-containing environment. Not surprisingly, both the number of transients and their stoichiometries have not changed compared to the previously suggested scheme (cf. Figures 1 and 12) because they are largely prescribed by the well-established overall stoichiometry of NO reduction[19,33]

$$e_{aq}^- + 3NO \rightarrow N_2O + NO_2^- \qquad (13)$$

by the number of observed reaction steps, and by their first-order dependencies on the NO concentration. However, the properties and reactivities that we assign to the intermediates are now completely different. The most important change is the recognition of different ground-state spin multiplicities for the conjugate ^{1}HNO/$^3NO^-$ acid−base pair that result in their spin-forbidden equilibration, which is slow even in buffers used in this work. Recently, we have addressed in significant detail the role of spin prohibition in this equilibration.[16] The lack of equilibration between $^3NO^-$ and ^{1}HNO gives rise to two separate reaction paths leading to the same intermediates and products, but on vastly different time scales.

The spectra of the intermediates have also been reevaluated. The only intermediate spectrum that can be cleanly observed in the pulse radiolysis experiments is that of $N_3O_3^-$ anion. The spectra previously assigned to the NO^- anion and to the $N_2O_2^-$ radical belong, in fact, to a mixture of species (mainly $N_2O_2^-$ and $N_3O_3^-$) and to the $N_3O_3^-$ anion, respectively. By plotting the maximum absorbance amplitude measured at 290 nm in 140 μM NO following an electron pulse vs pH, Grätzel and co-workers obtained a titration-like curve with an inflection point at pH 4.7, which they interpreted as the evidence for NO^- UV absorption and pK_a for HNO.[1] Although the species they were observing was actually not NO^- but principally $N_2O_2^-$; the question remains as to why they observed such a titration curve. The amount of promptly formed $N_2O_2^-$ is determined by the competition between NO and H^+ for e_{aq}^-, so the decrease in the $N_2O_2^-$ yield is expected at low pH. The pH dependence for this decrease is given by $F_1 = k_1[NO]/(k_1[NO] + k_H[H^+])$, where $k_H = 2.3 \times 10^{10}$ M^{-1} s^{-1} is the rate constant[28] for the $e_{aq}^- + H^+ \rightarrow$ H reaction. At 140 μM NO, F_1 describes a titration curve with half-height at pH 3.9. The second factor affecting absorption of $N_2O_2^-$ at low pH is its protonation, with p$K_a' = 5.5$, that yields HN_2O_2 whose molar absorptivity at 290

(33) Seddon, W. A.; Sutton, H. C. *Trans. Faraday Soc.* **1963**, *59*, 2323−2333.

nm is only one-half that of $N_2O_2^-$, as we have determined earlier.[17] The pH dependence of absorption due to both $N_2O_2^-$ and HN_2O_2 is given by $F_2 = (K_a' + 0.5[H^+])/(K_a' + [H^+])$, which has an inflection point at pH 5.5. The overall pH dependence of the absorption amplitude is given by the product F_1F_2 that also has typical shape of a titration curve. At 140 μM NO, it asymptotically approaches 0 at pH < 2 and 1 at pH > 7, reaching 0.5 at pH 4.7, exactly where Grätzel and co-workers observed an inflection point. Thus, the data obtained in this and our prior work[17] naturally explain the previous observations and pK_a assignment without invoking the UV absorption and protic equilibration of nitroxyl species.

Equation 8 has been extensively used in this work to deal with the pairs of consecutive first-order and pseudo-first-order reactions. However, the rate constants k' and k'' in this equation are known to be perfectly interchangeable if no restrictions are placed on the absorption amplitude A_2.[24] In other words, it is impossible to determine which of the two reactions is slower based on the observed transient absorption alone, and additional information, either mechanistic or spectral, is required to make the correct assignment. Because the rates of all but the last reactions in Figure 12 are linear in the NO concentration, the concentration dependencies are of little help.

For the sequence given by reactions 10, 4, and 5, the choice of reaction 5 as the slowest has been straightforward, for we have already established that $k_4 \gg k_{10}$ and determined the spectrum of $N_3O_3^-$; at sufficiently high NO concentration, the latter fully develops before its decay. Similarly, to identify the slower of reactions 3 and 4 occurring in series, one must independently know the spectrum of the $N_2O_2^-$ radical. Here, we have estimated that $k_4 \approx 2k_3$ solely on the basis of the degree of truncation of the $N_2O_2^-$ absorption given by eq 7, with $\epsilon_{290}(N_2O_2^-)$ taken from the $N_2O_2^-$ spectrum that we have previously obtained by the one-electron oxidation of the hyponitrite anion, $N_2O_2^{2-}$, in the absence of NO (Figure 2).[17] Implicit in this logic is the assumption that NO addition to $^3NO^-$ and one-electron oxidation of $N_2O_2^{2-}$ yield the same isomer of the $N_2O_2^-$ radical. In the latter case, the radical should retain its parent primary structure, which is the $ONNO^-$ bonded species. In the NO + $^3NO^-$ reaction, both $ONON^-$ and $NOON^-$ bonded isomers can also be envisioned, at least in principle. However, our data suggest that significant formation of these isomers in reaction 3 is unlikely, unless they exhibit essentially the same spectrum, as does the $ONNO^-$ isomer. This conclusion follows from the success of eq 7 in describing the observed amplitude truncation and from the similarity between the difference spectrum in Figure 7 and the spectrum of authentic $ONNO^-$ radical in Figure 2. We should also mention that $ONNO^-$ has been detected in both the gas phase[34,35] and inert cryogenic matrixes,[36−38] whereas neither of the other two isomers has ever been observed.

Chemically, $^3NO^-$ is a pseudohalide, and its addition to NO to give $(NO)_2^-$ represents a typical case of the so-called hemicolligation observed with many halides and pseudohalides [e.g., the I_2^- or $(SCN)_2^-$ radicals]. However, the amount of stabilization achieved in $(NO)_2^-$ is outstanding, particularly considering that two NO radicals do not measurably colligate at ordinary temperatures. Indeed, even the lower limit of $\sim 10^8$ M^{-1} for the equilibrium constant of reaction 3 found in our previous study[17] is at least 100 times larger than the value for any other reported hemicolligation equilibrium involving either halides or pseudohalides.[39] Notably, addition of an electron to a halogen, for example, to I_2, weakens the molecular bond by tenths of kilocalories per mole, whereas the opposite is true for $(NO)_2^-$. Also, in contrast to other halides and pseudohalides, another electron can be added to $(NO)_2^-$ to form the closed-shell $ONNO^{2-}$ anion, which is perfectly stable with respect to dissociation into two $^3NO^-$ anions. Quite likely, these unusual properties arise from the peculiar electronic structure of NO having two degenerate MOs that are occupied by a single electron. Splitting of these orbitals in the NO dimer should produce two bonding MOs, only one of which is filled, hence the extremely weak bonding. However, further consecutive addition of two more electrons will populate another bonding MO, which should result in the progressive stabilization of the dimer.

Acknowledgment. We thank Drs. Carol Creutz and Harold Schwarz for insightful comments. Research at Brookhaven National Laboratory was carried out under the auspices of the U.S. Department of Energy under Contract DE-AC02-98CH10886 from the Division of Chemical Sciences, Office of Basic Energy Sciences, and EMSP Grant #73824 (to S.V.L.). Work at New York University was supported by the NIH Grant 5R01 ES11589 and by a grant from the Kresge Foundation.

IC0501317

(34) Posey, L. A.; Johnson, M. A. *J. Chem. Phys.* **1988**, *88*, 5383−5395.
(35) Li, R.; Continetti, R. E. *J. Phys. Chem. A* **2002**, *106*, 1183−1189.
(36) Andrews, L.; Zhou, M. F.; Willson, S. P.; Kushto, G. P.; Snis, A.; Panas, I. *J. Chem. Phys.* **1998**, *109*, 177−185.
(37) Andrews, L.; Zhou, M. F. *J. Chem. Phys.* **1999**, *111*, 6036−6041.
(38) Lugez, C. L.; Thompson, W. E.; Jacox, M. E.; Snis, A.; Panas, I. *J. Chem. Phys.* **1999**, *110*, 10345−10358.
(39) Stanbury, D. M. In *General Aspects of the Chemistry of Radicals*; Alfassi, Z. B., Ed.; Wiley: New York, 1999; pp 347−384.